# "Antiflow" of Antiprotons in Heavy Ion Collisions

A. Jahns, C. Spieles, H. Sorge, H. Stöcker, and W. Greiner
*Institut für Theoretische Physik, Johann Wolfgang Goethe Universität, Frankfurt am Main, Germany*
(Received 20 December 1993)

In the framework of the relativistic quantum molecular dynamics approach we investigate antiproton ($\bar{p}$) observables in Au+Au collisions at 10.7$A$ GeV. The rapidity dependence of the in-plane directed transverse momentum $\mathbf{p}_x(y)$ of $\bar{p}$'s shows the opposite sign of the nucleon flow, which has indeed recently been discovered at 10.7$A$ GeV by the E877 group. The "antiflow" of $\bar{p}$'s is also predicted at 2$A$ GeV and at 160$A$ GeV and appears at all energies also for $\pi$'s and $K^-$'s. These predicted $\bar{p}$ anticorrelations are a direct proof of strong $\bar{p}$ annihilation in massive heavy ion reactions.

PACS numbers: 25.75.+r

Antibaryons ($\bar{B}$) have a large annihilation cross section in baryon-rich environments formed in heavy ion reactions. By studying their production and absorption mechanisms we hope to get information about the time evolution of the baryon density in the reaction region [1–4].

In previous calculations [5] experimental antiproton ($\bar{p}$) data in the energy regime of the BNL Alternating Gradient Synchrotron (AGS) have been explained on a microscopic level. The final particle yields have been interpreted in terms of two counterbalancing effects: On the one hand, $\bar{B}$ *production* is enhanced due to collective effects; on the other hand, $\bar{B}$ *annihilation* becomes stronger due to nuclear stopping and therefore the baryon density increases. The strength of these competing processes depends strongly on the incident energy and the reaction volume.

Recent measurements of inclusive $\bar{p}$ spectra with proton, silicon, and gold beams at the AGS (10–15$A$ GeV) [6–10] do not give clues about the strength of such opposite effects. These results—with an uncertainty of a factor 2 in the $\bar{p}$ yields as extrapolated from $pp$ collisions—are compatible with relativistic quantum molecular dynamics (RQMD) calculations as well as with the first collision model: Antibaryons are produced similar to the first collision yields if the absorption is neglected. There are other theoretical calculations which predict that $\bar{B}$ are also enhanced in a quark-gluon plasma event [11], by chiral symmetry restoration [12], in-medium effects [13], or by string-string interactions [14].

In this Letter we demonstrate that strong annihilation distorts considerably the momentum distribution of antibaryons. Because of the buildup of a high density and pressure zone, the nucleons stemming from the projectile bounce off in the reaction plane just into the opposite direction of the target nucleons in noncentral collisions. Antibaryons—and also pions and negatively charged kaons—show as a result of rescattering and absorption a strong "antiflow", i.e., anticorrelations to the nucleons in the reaction plane. This leads to an observable asymmetry in the azimuthal angular distributions ($dN_{\bar{p}}/d\phi$) or in the mean directed transverse momentum of antiprotons in the reaction plane as a function of the rapidity $\mathbf{p}_x(y)$. This can be experimentally tested once the reaction plane is determined, e.g., by measuring the azimuthal distribution of forward and backward going baryons or transverse energy in the same event in which the $\bar{p}$'s are detected. First experimental evidence for the collective flow [15] has recently been reported by the E877 group [16]. Further on, correlations between particle production and transverse momenta of projectile fragments have been demonstrated by the E802 collaboration [17]. Azimuthal asymmetries for the $\pi^{\pm}/p$ and $(d+t)/p$ ratios have been found in the target rapidity region. Measurements of $\bar{p}$ correlations are in progress [18,19].

The calculations presented here are based on a microscopic phase space approach, the relativistic quantum molecular dynamics model (RQMD 1.07, cascade mode). Let us briefly describe the relevant features of this model [20,21]. The fate of all particles—the original as well as the newly produced ones—is followed in RQMD by propagating those particles on classical trajectories and allowing collisions between all of them until the cascade process is finished. The interaction probabilities are given by geometry, i.e.; the minimum two-body c.m.-system (c.m.s.) distance has to be below $\sqrt{\sigma/\pi}$ with $\sigma$ the binary reaction cross section. The dominant reaction mechanism in the first stage of a reaction when projectile and target interpenetrate each other is the excitation of both collision partners to resonances or strings. Strings are a 1+1 dimensional idealization of the chromoelectric flux tube with constituent quarks moving at their ends. The decay of the excited states depends on its mass. If the mass is below some threshold, e.g., for nonstrange baryon resonances 2 GeV/$c^2$, they are projected onto the experimentally given resonance spectrum. Higher mass states fragment as color strings. The string fragmentation parameters are universal for soft hadronic multiparticle production and extracted from $e^+e^-$ and $lh$ collisions.

A second source for excitation of baryons which is of utmost importance at AGS energy as discussed in [5,21] are secondary interactions, the dominant process being the annihilation of produced mesons on baryons which leads to the formation of $s$ channel resonances or strings. The formation time of newly produced secondaries is


0031-9007/94/72(22)/3464(4)$06.00

given by the finite lifetime of a resonance or by the time which a string needs to break into parts which is given by the momenta of the fragments. Those resonances formed are not only responsible for strangeness enrichment [21], but they may be further excited in a subsequent collision to a mass larger than $3m_N$ which allows for $\bar{N}N$ creation. Such multistep processes have to be viewed as a complicated interplay between excitation and decay processes [5]. Further on, the free $N\bar{N}$ annihilation cross section enters into the RQMD calculations.

We have studied Au+Au reactions both at 10.7$A$ GeV and also at 2$A$ GeV and 160$A$ GeV. In accord with recent $\bar{p}$ measurements without centrality trigger [18], we focus here on minimum bias calculations. We want to point out, however, that much more detailed information can be obtained if impact parameter selection criteria are applied, as was clearly demonstrated in the $E \sim 1A$ GeV energy domain [22–24].

It is expected that multistep processes might become even more important for large mass target-projectile combinations due to the larger reaction volume and lifetime. Note that the Au beam energy is closer to the $\bar{p}$ production threshold than for the Si beam energy at the AGS. Therefore, additional production processes—apart from first collisions—should become even more important. On the other side, high nuclear density—caused by strong nuclear stopping—should strengthen the $\bar{p}$ suppression. In contrast, a microscopic calculation with the cascade model ARC [25] was presented in which such multistep processes are less important, because the excitation spectrum is restricted to the $\Delta$ mass only. Instead, in a high density environment the annihilation of antiprotons is suppressed.

Figure 1 shows the calculated rapidity distribution of the antiprotons, $dN_{\bar{p}}/dy$, for minimum bias Au(10.7$A$ GeV)+Au reactions with (solid histogram) and without annihilation (dotted histogram). RQMD calculations are also given for the $\bar{p}$ distributions in $pp$ reactions. This distribution (solid curve) is multiplied by the calculated number of first nucleon-nucleon collisions ($\sim$12 Fermi momentum considered) in Au+Au. The initially produced $\bar{p}$ yield in the full RQMD calculation is a factor of 20 higher than in the first collision mode. Even after annihilation is included, this factor is still 2 (i.e., the model predicts $\approx 90\%$ annihilation). Hence, we infer that in heavy systems like gold on gold the enhanced production of antibaryons is *not* counterbalanced by the annihilation.

The absorption is strongest around midrapidity. The final $dN_{\bar{p}}/dy$ distribution is broader than expected for antiprotons which originate from first $pp$ reactions, because $\bar{B}$ annihilation is correlated with the rapidity density of baryons which is highest at midrapidity. This goes along with large baryon stopping. Preliminary data measured at $p_t = 0$ [26] seem to exhibit this broadening of the $dN_{\bar{p}}/dy$ distribution. This supports the scenario presented here. The antiproton yield should also be measured in small systems ($pp$, Si+Si, etc.)—in addition to Au+Au

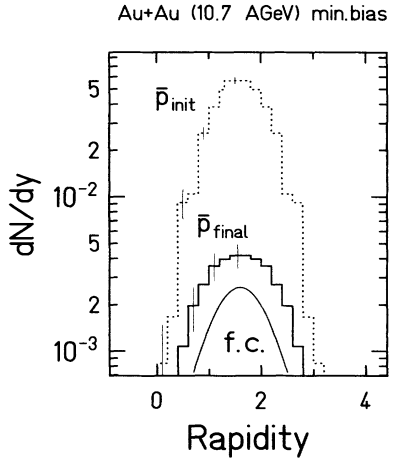


FIG. 1. The antiproton rapidity distribution $dN_{\bar{p}}/dy$ is shown for minimum bias Au+Au collisions at 10.7$A$ GeV. The two histograms represent the RQMD results with (solid) and without (dotted) annihilation. The solid curve corresponds to the $\bar{p}$ calculated in $pp$ collisions multiplied by 12 (number of first collisions in minimum bias Au+Au reactions). The Fermi momentum is also considered.

—at the same energy. A systematic study of the mass and centrality dependence of antiproton production can help to disentangle the competing effects of multistep production and enhanced absorption predicted in the present work.

One can look at observables which exhibit collective behavior more clearly. For instance, baryon stopping and creation of a baryon dense region may lead to collective baryon flow predicted a long time ago on the basis of the fluid-dynamical model [22]. The observation of flow is in turn of vital importance for diagnostic purposes: The predicted bounceoff and squeezeout effects can be used as barometers to measure the pressure buildup in the hot and dense participant matter. The bounceoff can be quantified, e.g., via the measurement of the directed in-plane transverse momentum transfer which has been widely used at energies of the Bevalac at LBL or the SIS at GSI Darmstadt [23,24]. While the nucleonic flow at target and projectile rapidity, respectively, can easily be pictured as repelled and deflected matter, the antibaryons will show an anticorrelated behavior due to annihilation and rescattering.

Figure 2 shows this behavior for a medium impact parameter ($b = 6$ fm): a snapshot of the baryon density contours in the reaction plane after 16 fm/$c$ (c.m.s.). The antiproton momenta are represented by the arrows. Obviously "antimatter" goes in the opposite direction to "matter."

Which observables are relevant to quantify this effect? One possibility is to look for the azimuthal ($\phi$) distribution of antiprotons. $\phi$ is the angle between $\mathbf{p}_T$ and the $x$ axis ($\tan\phi = |p_y|/p_x$). Thus, a vector with $\phi = 0°$ points in the direction of the $x$ axis. Strong antibaryon annihilation leads to a decreasing $dN/d\phi$ distribution when going

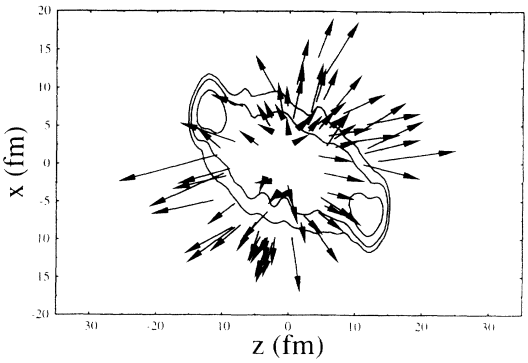


FIG. 2. Snapshot (after 16 fm/$c$) in the reaction plane for semiperipheral ($b=6$ fm) Au+Au collisions at 10.7$A$ GeV. Shown are RQMD calculations for the baryon density (contour plots) and antiprotons (arrows). The lengths of the arrows represent the momenta of the particles, projected on the reaction plane. $\bar{p}$ are obtained from $10^4$ (overlayed) events.

from 0° to 180°. If annihilation is turned off, this distribution is flat: The antiprotons are—in the present model—produced azimuthally isotropic. The $\bar{p}$ yield in a given rapidity bin (in percent) which goes to the upper hemisphere ($\phi<90°$, $p_x>0$) is shown in Fig. 3 as a function of rapidity for Si+Au ($b=3.5$ fm) and Au+Au (minimum bias).

Up to 70% of the antiprotons exhibit $\phi<90°$ at target rapidity for both systems. This means more antiparticles survive if they are emitted in opposite directions than the matter flow. This effect disappears at projectile rapidity for Si+Au due to the stopping of the Si projectile.

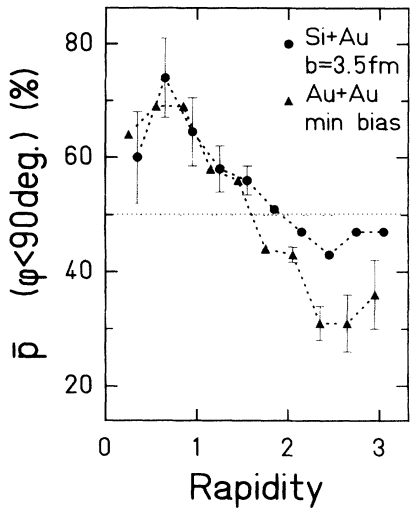


FIG. 3. Percentage of final antiprotons with an azimuthal angle $<90°$. Analyzed are the systems Si+Au ($b=3.5$ fm) and Au+Au (minimum bias) at AGS energies with RQMD. At target rapidity both systems show an azimuthal asymmetry up to 70%. At projectile rapidity this effect disappears for Si+Au due to stopping of the Si projectile.

Figure 4 shows the in-plane directed transverse momentum $\mathbf{p}_x(y)$ as a function of rapidity for all produced negatively charged particles (divided by the particles mass). Minimum bias events are calculated. To demonstrate the antiflow the corresponding curve for protons is added (see Ref. [27]). Rescattering also modifies the $\pi^-$ and $K^-$ distributions from the primary nucleon-nucleon collisions. At lower energies this anticorrelation of pions to the nucleons can be explained by pion absorption [28] or by multiple $\pi N$ scattering [29]—the observed pions in the target-projectile rapidity frame are reflected from the spectator pieces. The latter argument is not relevant for antibaryons.

Nucleon flow is predicted for SIS, AGS, and CERN SPS energies [15]. Antiflow of antinucleons is also obtained for SIS energies ($E_{\rm lab}\sim 2A$ GeV) and for the CERN Pb beam energies ($E_{\rm lab}\sim 160A$ GeV) as demonstrated in Fig. 5. The directed transverse momentum of the $\bar{p}$'s at projectile and target rapidity is most prominent for low energies. This goes along with the annihilation rate, which rises with decreasing energy [30]. Note that at subthreshold energies antiproton production takes place dominantly in central collisions. At the AGS energy regime—considering the amount of flow and the statistics—a confirmation of our predictions seems favorable at $0.4\le y\le 1.2$ (at $2.0\le y\le 2.8$ for protons). This rapidity region is accessible by recent measurements.

In Figs. 4 and 5 the transverse momentum is shown relative to the original beam axis. In order to improve

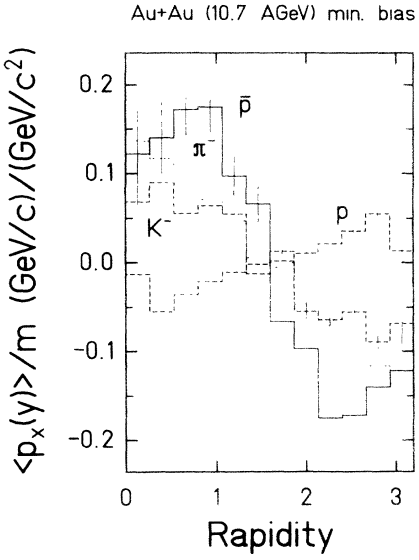


FIG. 4. Directed in-plane transverse momentum for different particles ($\bar{p},p,\pi^-,K^-$) in the reaction Au+Au (minimum bias) at 10.7$A$ GeV divided by the particle masses as a function of rapidity $\langle p_x(y)/m\rangle$. The flow effect of antiprotons is in the mean 7 times larger than for $\pi^-$ or $K^-$. For the $\bar{p}$ about $10^5$ events are generated. This leads to $\sim$15% statistical error for the relevant rapidity bins $0.4\le y\le 1.2$ (at $2.0\le y\le 2.8$ for protons).

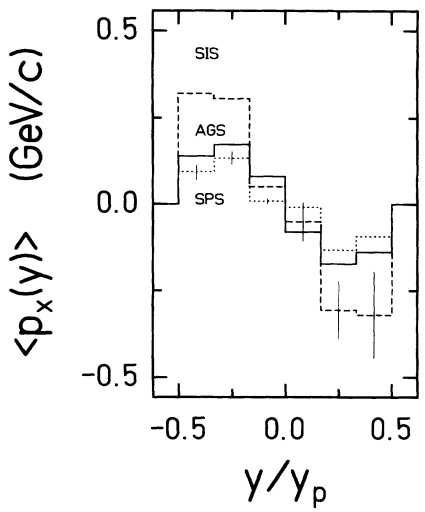


FIG. 5. Directed in-plane transverse momentum for antiprotons in minimum bias reactions at SIS (Au+Au at $E_{lab}\sim 2A$ GeV), AGS (Au+Au at $E_{lab}\sim 11A$ GeV), and CERN SPS (Pb+Pb at $E_{lab}\sim 160A$ GeV) energies as a function of the scaled rapidity ($y/y_P$).

statistics every event for symmetric systems has been reflected around midrapidity. This explains the exact reflection symmetry in Figs. 4 and 5. Note that the numerical code reproduces symmetric results for symmetric systems within statistical accuracy.

In conclusion, the predicted antiflow of antiprotons can help to verify strong antibaryon annihilation in massive heavy ion collisions. The experimental discovery of this anticorrelation would rule out the first chance collision model with screening of antibaryon annihilation, which has recently been put forward to explain experimental data.

[1] P. Koch and C. Dover, Phys. Rev. C **40**, 195 (1989).
[2] H. Sorge, A. v. Keitz, R. Mattiello, H. Stöcker, and W. Greiner, Phys. Lett. B **243**, 7 (1990).
[3] S. Gavin, M. Gyulassy, M. Plümer, and R. Venugopalan, Phys. Lett. B **234**, 175 (1990).
[4] A. Jahns, C. Spieles, R. Mattiello, H. Sorge, H. Stöcker, and W. Greiner, Nucl. Phys. **A566**, 483c (1994).
[5] A. Jahns, H. Stöcker, W. Greiner, and H. Sorge, Z. Phys. A **341**, 243 (1992); Phys. Rev. Lett. **68**, 2895 (1992); A. Jahns, C. Spieles, R. Mattiello, H. Stöcker, W. Greiner, and H. Sorge, Phys. Lett. B **308**, 11 (1993).
[6] E814 Collaboration, J. Barette *et al.*, Phys. Rev. Lett. **70**, 1763 (1993).
[7] E858 Collaboration, A. Aoki *et al.*, Phys. Rev. Lett. **69**, 2345 (1992).
[8] E802 Collaboration, T. Abbot *et al.*, Phys. Lett. B **271**, 447 (1991).
[9] E802 Collaboration, T. Abbott *et al.*, Phys. Rev. C **47**, R1351 (1993).
[10] E886 Collaboration, G. Diebold *et al.*, Phys. Rev. C **46**, 2984 (1993).
[11] U. Heinz, P. R. Subramanian, H. Stöcker, and W. Greiner, J. Phys. G **12**, 1237 (1986).
[12] J. Ellis, U. Heinz, and H. Kowalski, Phys. Lett. B **233**, 233 (1989).
[13] J. Schaffner, I. N. Mishustin, L. M. Satarov, H. Stöcker, and W. Greiner, Z. Phys. A **341**, 47 (1991).
[14] H. Sorge, M. Berenguer, H. Stöcker, and W. Greiner, Phys. Lett. B **289**, 6 (1992).
[15] H. Sorge, A. v. Keitz, R. Mattiello, H. Stöcker, and W. Greiner, Nucl. Phys. **A525**, 95C (1991); A. v. Keitz, L. Winckelmann, A. Jahns, H. Stöcker, and W. Greiner, Phys. Lett. B **263**, 353 (1991).
[16] E877 Collaboration, P. Braun-Munzinger *et al.*, in *Proceedings of NASI Hot Dense Nuclear Matter, Bodrum, Turkey, 1993* (Plenum, New York, 1993).
[17] E802 Collaboration, T. Abbott *et al.*, Phys. Rev. Lett. **70**, 1393 (1993).
[18] E886 Collaboration, G. Diebold *et al.* (private communication).
[19] P. Rotshild and S. Nagamiya (private communication).
[20] H. Sorge, H. Stöcker, and W. Greiner, Ann. Phys. (N.Y.) **192**, 266 (1989).
[21] R. Mattiello, H. Sorge, H. Stöcker, and W. Greiner, Phys. Rev. Lett. **63**, 1459 (1989); H. Sorge, R. Mattiello, A. Jahns, H. Stöcker, and W. Greiner, Phys. Lett. B **271**, 37 (1991); H. Sorge, R. Mattiello, H. Stöcker, and W. Greiner, Phys. Rev. Lett. **68**, 286 (1992).
[22] H. Stöcker and W. Greiner, Phys. Rep. **137**, 277 (1986).
[23] H. A. Gustafson, H. H. Gutbrod, B. Kolb, H. Loehner, B. Ludewigt, A. M. Poskanzer, T. Renner, H. Riedesel, H. G. Ritter, A. Warwick, F. Weik, and H. Wieman, Phys. Rev. Lett. **52**, 1590 (1984).
[24] R. E. Renfordt, D. Schall, R. Bock, R. Brockmann, J. W. Harris, A. Sandoval, R. Stock, H. Stroebele, D. Bangert, W. Rauch, G. Odinec, H. G. Pugh, and L. S. Schroeder, Phys. Rev. Lett. **53**, 763 (1984).
[25] S. H. Kahana, Y. Pang, T. Schlagel, and C. B. Dover, Phys. Rev. C **47**, R1356 (1993).
[26] E858/878 Collaboration, B. Shiva Kumar *et al.*, Nucl. Phys. **A566**, 439c (1994).
[27] R. Mattiello, A. Jahns, H. Sorge, H. Stöcker, and W. Greiner, UFTP Report No. 352/1994 (to be published).
[28] B. A. Li, W. Bauer, and G. F. Bertsch, Phys. Rev. C **44**, 2095 (1991).
[29] S. A. Bass, C. Hartnack, R. Mattiello, H. Stöcker, and W. Greiner, Phys. Lett. B **302**, 381 (1993).
[30] C. Spieles, A. Jahns, H. Sorge, H. Stöcker, and W. Greiner, Mod. Phys. Lett. A **27**, 2547 (1993).